# Thermo-responsive Non-Woven Scaffolds for "Smart" 3D Cell Culture

Claire L Rossouw[a,c*], Avashnee Chetty[b], F Sean Moolman[b], Lyn-Marie Birkholtz[c], Heinrich Hoppe[c,d], Dalu T Mancama[a]

[a]Biosciences, CSIR, PO Box 395, Pretoria, 0002 , South Africa

[b]Materials Science and Manufacturing, CSIR, PO Box 395, Pretoria, 0002, South Africa

[c]Department of Biochemistry, University of Pretoria, Private Bag X20, Hatfield, 0028, South Africa

[d]Department of Biochemistry, Microbiology & Biotechnology, Rhodes University, P.O. Box 94 Grahamstown, 6140, South Africa

*Corresponding author, E-mail: crossouw@csir.co.za, Tel: +27 12 841 3272, Fax: +27 12 841 3651

**Running Title:** "Smart" 3D Cell Culture

Accepted in "Biotechnology and Bioengineering"

## Abstract

The thermo-responsive polymer poly(*N*-isopropylacrylamide) has received widespread attention for its *in vitro* application in the non-invasive, non-destructive release of adherent cells on two dimensional surfaces. In this study, 3D non-woven scaffolds fabricated from poly(propylene) (PP), poly(ethylene terephthalate) (PET) and nylon that had been grafted with PNIPAAm were tested for their ability to support the proliferation and subsequent thermal release of HC04 and HepG2 hepatocytes. Hepatocyte viability and proliferation was estimated using the Alamar Blue assay and Hoechst 33258 total DNA quantification. The assays revealed that the pure and grafted non-woven scaffolds maintained the hepatocytes within the matrix and promoted 3D proliferation comparable to that of the commercially

available Algimatrix™ alginate scaffold. Albumin production and selected cytochrome P450 genes expression was found to be superior in cells growing on pure and grafted non-woven PP scaffolds as compared to cells grown as a 2D monolayer. Two scaffolds, namely, PP-*g*-PNIPAAm-A and PP-*g*-PNIPAAm-B were identified as having far superior thermal release capabilities; releasing the majority of the cells from the matrices within 2 h. This is the first report for the development of 3D non-woven, thermo-responsive scaffolds able to release cells from the matrix without the use of any enzymatic assistance or scaffold degradation.

**Keywords**

Poly(*N*-isopropylacrylamide), Poly(propylene), cell proliferation, hepatocyte, Non-woven fabric

## 1. Introduction

Cells growing *in vitro* are traditionally grown on two-dimensional (2D) surfaces of tissue culture plastic and bear little resemblance to the complexities of the three-dimensional (3D) tissues from which they are derived (Bokhari et al., 2007b). Two-dimensional monolayer cultures are convenient for routine work but impose unnatural geometric and mechanical constraints upon the cells. The inherent problem with cells growing on 2D surfaces is the lack of dorsal anchorage points, which affects the balance between cells spreading or retracting. This creates an unnatural stimulatory environment for the cells resulting in an imbalance which causes the aberrant spreading of the cells (Bokhari et al., 2007a).

In native tissue, cells connect to each other as well as to the extracellular matrix (ECM). Various culture applications have shown that the growth and function of cells as multi-cellular, 3D structures is significantly different and more representative of the physiological state compared to 2D monolayer cultures (Beningo et al., 2004; Bokhari et al., 2007b; Cukierman et al., 2001; Schmeichel and Bissell, 2003; Witte and Kao, 2005). The difference lies in the formation of chemical signal or molecular gradients which are important for biological differentiation, cell fate, organ development and signal transduction to name but a few. Other changes in metabolic and gene expression patterns as well as a significant reduction in the production of ECM proteins have been observed for 2D monolayer cultures (Zhang, 2004). A change of environment for the cells, therefore, translates into a change in function and capacity for growth and differentiation. These enhanced interactions in the 3D environment enable the cells to interpret the multitude of biochemical and physical cues from the immediate environment (Bokhari et al., 2007a). This insight into cell phenotype and function *in vitro* and the desire to have cells functioning closely to their *in vivo* counterparts has intensified the demand for the best materials able to support 3D cell growth.

Extensive research has been conducted on the use of thermo-responsive, "smart" polymers for non-invasive cell harvesting over the past three decades. A temperature-sensitive polymer, poly-(*N*-isopropylacrylamide) (PNIPAAm), has been covalently grafted onto polystyrene cell culture tray surfaces to facilitate cell attachment and trypsin-independent cell release induced by a temperature change (Okano et al., 1995). PNIPAAm switches reversibly between hydrophobic and hydrophilic states when the temperature crosses its lower critical solution temperature (LCST) of approximately 32°C. This allows cells to attach onto the PNIPAAm surface at 37°C when the surface is hydrophobic while spontaneously releasing cells from the hydrophilic surface at 25°C (Okano et al., 1995). The major advantage of using

PNIPAAm in cell culture is that cells are non-invasively harvested as intact cell sheets with critical cell surface proteins, growth factor receptors, and cell-to-cell junction proteins remaining intact (Curti et al., 2005; Kushida et al., 1999; Yamato et al., 2001).

With much effort being dedicated to the fabrication and testing of materials that can support 3D cell growth (including biodegradable polymers, hydrogels and inert solid scaffolds), this study proposes combining the two technologies to create a novel 3D non-woven scaffold grafted with PNIPAAm for simple non-invasive cell harvesting. As we demonstrate, this new technology creates an enhanced environment where cells can grow in 3D thereby benefitting from the proposed advantages of this morphological state and, furthermore, release/harvesting of cells in a 3D conformation is achieved non-enzymatically through temperature changes.

## 2. Materials and Methods

### 2.1. Scaffold fabrication

Three different non-woven polymer scaffolds were investigated in this study as substrates for cell proliferation. Fabrics made from poly(propylene) (PP) and poly(ethylene terephthalate) (PET) non-woven polymers with a median flow pore (MFP) size of 150-300 μm were developed based on needle-punching technology. The non-woven mats used as scaffolds were thermo-fused at 145°C and 180°C respectively in order to prevent the dissociation of the fibres during cell culture. Nylon non-woven scaffolds with pores sizes in the range of 40-80 μm were developed due to the lower fibre density of the nylon compared to PP and PET fibres, and thermofused at 200°C. Scaffolds were characterised for porosity, water

permeability, compressibility, fabric density, tensile strength, area weight and thickness (A, Chetty, data not presented). Algimatrix™ alginate scaffolds (Invitrogen, Eugene, Oregon, USA) were included as a comparison.

### 2.2. Grafting methods

PP, PET and nylon non-woven scaffolds were grafted with PNIPAAm using a solution free-radical polymerisation (SFRP) technique. Briefly, the grafting methods investigated involved swelling of pure (or functionalised) non-woven scaffolds in an initiator solution followed by SFRP in an aqueous NIPAAm monomer solution with heat activation (70ºC or 50ºC). Two functionalisation methods were investigated prior to grafting, i.e. oxyfluorination (performed using a proprietary method at Pelchem (Pty) Ltd, South Africa) or a chemical oxidation method using APS. Grafting of PNIPAAm onto the surface of the fibres was confirmed by attenuated total reflection-fourier transform infrared spectroscopy (ATR-FTIR)**,** differential scanning calorimetry (DSC), X-ray photoelectron spectroscopy (XPS) and scanning electron microscopy (A. Chetty, manuscript under review).

### 2.3. Cell-scaffolds interaction

HC04 (MRA-156, MR4, ATCC® Manassas, Virginia) and HepG2 (ATCC HB-8065™, ATCC®) hepatocyte cell lines were used in the study. HC04 cells are human hepatocytes immortalised by Sattabongkot and colleagues (Sattabongkot et al., 2006) from healthy human primary liver cells to support the *in vitro* development of human malaria species. HepG2 cells are human hepatocellular liver carcinoma cells routinely used worldwide for *in vitro* liver studies. Scaffolds of size 5 mm x 5 mm x 3 mm were sterilised in 70% ethanol for 1 h, rinsed

three times in 1xPBS and allowed to dry in a laminar hood. The scaffolds were soaked overnight at 37 °C in the cell culture media specific for the cell line used, to reduce any surface tension effects (Wagner et al., 1997) as well as to ascertain whether the scaffolds had been effectively sterilised, prior to seeding the non-woven scaffolds with the hepatocytes. HepG2 cells were cultured in Dulbecco's Modified Eagle Medium (DMEM, Lonza Walkersville, Inc. Maryland, USA) with 2 mM L-glutamine and supplemented with 10% (v/v) foetal calf serum (FCS), 100 g $mL^{-1}$ penicillin and 10 μg $mL^{-1}$ streptomycin (Sigma-Aldrich Chemie, GmbH, Steinheim, Germany). HC04 cells were cultured in 1:1 DMEM:Hams F12 media (Lonza) with 2 mM L-glutamine and supplemented with 10% (v/v) FCS, 100 g $mL^{-1}$ penicillin and 10 μg $mL^{-1}$ streptomycin (Sigma-Aldrich Chemie). HC04 and HepG2 hepatocytes growing in culture flasks were trypsinized and resuspended to a concentration of 1 x $10^6$ cells $mL^{-1}$. A 200 μL aliquot of this cell suspension was gently dripped onto each of the non-woven and Algimatrix™ scaffolds in a 96-well plate, resulting in a final concentration of 2 x $10^5$ cells seeded into each scaffold.

The scaffolds were incubated at 37°C for 2 h to allow the cells to attach to the scaffolds. Thereafter, the scaffolds were removed from the 96-well tissue culture plate using sterile tweezers and placed into the well of a 12-well tissue culture plate with 2 mL media and cultured under standard conditions. Scaffolds containing the HepG2 and HC04 hepatocytes were maintained in culture for a period of 21 days with media changes performed every 48 h.

### 2.3.1. Cell viability and proliferation

#### 2.3.1.1 Alamar Blue assay

The Alamar Blue (AB) assay (Promega, Madison, WI), a fluorometric indicator of cell metabolic activity, was performed to determine cell viability and proliferation. The cell-scaffold constructs were removed from the culture plates on day 0 (estimation of cell retention in the scaffolds), 3, 7, 11, 14 and 21 post-seeding. Scaffolds (n=5) were gently washed with PBS, re-fed with 450 µL medium and 50 µL AB dye and incubated for 30 min at 37°C. Fluorescence was measured at room temperature with a GENios Fluorimeter (TECAN, Männedorf, Switzerland) at excitation and emission wavelengths of 520 nm and 590 nm, respectively. A cell number was obtained through a calibration curve derived by correlating a known cell number (determined by counting in a haemocytometer) with the fluorescence intensity of the solution.

#### 2.3.1.2 DNA quantification using Hoechst 33258

Hoechst 33258 (Invitrogen) is a bisbenzimide DNA intercalator which binds to the A+T-rich regions of double stranded DNA and was used to quantify cellular DNA accumulation on the scaffolds. 3D cell-scaffolds (n=5) were washed in PBS, frozen and thawed in 500 µL of distilled water at 37°C for 1 h and cell lysis further ensured by three consecutive freeze-thaw cycles. Fluorescence was measured on a FL$_X$800 microplate fluorescence reader (Bio-Tek Instruments, Inc., Vermont, USA) using equal volumes cell lysates and Hoechst 33258 dye solution (20 µg $mL^{-1}$). Hoechst 33258 excites in the near UV (350 nm) and emits in the blue

region (450 nm). The number of viable cells per scaffold was calculated by extrapolation from a calibration curve that was generated as described in Rago and colleagues (1990).

### 2.3.2. Imaging cell-scaffold-interaction

Cells were visualised on the scaffolds using fluorescein diacetate (FDA, Sigma-Aldrich Chemie) as described by Dvir-Ginsberg and colleagues (2003). Essentially, the non-specific esterase activity in the cytoplasm of viable cells converts non-fluorescent FDA to fluorescein, a green fluorescent dye. Cell-scaffolds were incubated in FDA for 5 min and rinsed in PBS. Both the top and bottom of the scaffolds were viewed 3, 7, 11, 14 and 21 days post seeding. Visualisation was performed at 40x magnification using a standard fluorescence microscope (Olympus BX41, Olympus Microscopy, Essex, UK) equipped with a 490 nm bandpass filter with a 510 nm cut-off filter for fluorescence emission.

### 2.3.3. Hepatocyte metabolic activity

#### 2.3.3.1 Albumin assay

Albumin production was used to establish hepatocyte metabolic activity when growing in 3D versus 2D. Pure PP (un-grafted scaffolds, mean pore size of 200 µm) were punched into disks (15 mm in diameter and 3 mm thick) and seeded with 1.5 x $10^6$ HC04 or HepG2 hepatocytes and cultured for 21 days; medium changes were performed every 24 h. 24 h culture supernatant samples were collected for albumin quantification on days 3, 7, 10, 14 and 21. The 24 h culture supernatant from a 70% confluent 75 $cm^2$ flask of HC04 or HepG2 hepatocytes was used as the 2D comparison. Levels of albumin secreted into the media were determined using the Albumin Fluorescence Assay Kit (Sigma-Aldrich) and normalised to

total protein in the media as determined by the Bradford assay. Statistical analysis was performed using a paired t-test of unequal variance where $p< 0.01$ and $p<0.05$.

#### 2.3.3.2 Cytochrome P450 mRNA expression

Pure PP non-woven scaffolds with a mean pore size of 200 μm seeded with HC04 hepatocytes (as in section 2.3.3.1) were frozen away on days 10, 14 and 21 post-seeding. Scaffolds seeded with HepG2 hepatocytes were frozen away on day 21 post-seeding. To investigate the effect of scaffold pore size and grafting on gene expression, PP-*g*-PNIPAAm scaffolds with mean pore sizes of 100 μm, 150 μm, 200 μm (PP-*g*-PNIPAAm-B1, B2 and B3; Table 1) were seeded with HC04 hepatocytes and frozen away on day 21 post-seeding. Hepatocytes growing in a control 75 $cm^2$ cell culture flask were harvested at 70% confluence and frozen at -80°C until further use. RNA extractions were performed as described by Clark et al., (2008) and cDNA-synthesis was performed using the high-capacity RNA-to-cDNA Kit (Applied Biosystems, Foster City, CA, USA). Cytochrome P450 (CYP) *2C19*, *2C9*, *1A2*, *2D6*, *3A4* and *3A5* mRNA expression levels were determined using quantitative real time-PCR (qRT-PCR). The qRT-PCR was conducted according to manufacturer's instructions (Life Technologies Corporation, Carlsbad, CA, USA) with an annealing temperature of 60°C. Relative quantification of gene expression levels was determined using the comparative Ct method ($2^{-\Delta\Delta Ct}$) (Livak and Schmittgen, 2001) and normalised to the β-actin gene (Sainz et al., 2009). Statistical analysis was performed as described in 2.3.3.1.

| Sample Name | Polymer | | | Grafting method | | | | |
|---|---|---|---|---|---|---|---|---|
| | Polymer | MFP (μm) | Mass (g/m²) | Pre-treatment | Initiator | NIPAAm added | Temp (°C) | Time (h) |
| PP-Cont | PP | 127 | - | - | - | - | - | - |
| PET-Cont | PET | 127 | - | - | - | - | - | - |
| Nylon-Cont | Nylon | 40-80 | - | - | - | - | - | - |
| PP-*g*-PNIPAAm-1 | PP | 127 | - | APS[1] | Ceric ion/nitric acid | ✓ | 70 | 24 |
| PP-*g*-PNIPAAm-1a | PP | 127 | - | APS | Ceric ion/nitric acid | ✓ | 50 | 24 |
| PP-*g*-PNIPAAm-2 | PP | 127 | - | - | APS | ✓ | 70 | 24 |
| PET-*g*-PNIPAAm-2 | PET | 127 | - | - | APS | ✓ | 70 | 8 |
| PP-*g*-PNIPAAm-A | PP | 127 | - | Oxyfluorination[2] | APS | ✓ | 70 | 7 |
| PP-*g*-PNIPAAm-B (Test 1) | PP | 127 | - | Oxyfluorination[3] | APS | ✓ | 70 | 7 |
| PET-*g*-PNIPAAm-A | PET | 127 | - | Oxyfluorination[2] | APS | ✓ | 70 | 7 |
| PET-*g*-PNIPAAm-B | PET | 127 | - | Oxyfluorination[3] | APS | ✓ | 70 | 7 |
| Nylon-*g*-PNIPAAm-A | Nylon | 40-80 | - | Oxyfluorination[2] | APS | ✓ | 70 | 7 |
| Nylon-*g*-PNIPAAm-B | Nylon | 40-80 | - | Oxyfluorination[3] | APS | ✓ | 70 | 7 |
| Thermal Release: Pore Size | | | | | | | | |
| PP-*g*-PNIPAAm-B1 | PP | 100 | 200 | Oxyfluorination[3] | APS | ✓ | 70 | 7 |
| PP-*g*-PNIPAAm-B2 | PP | 150 | 100 | Oxyfluorination[3] | APS | ✓ | 70 | 7 |
| PP-*g*-PNIPAAm-B3 | PP | 200 | 95 | Oxyfluorination[3] | APS | ✓ | 70 | 7 |
| Thermal Release: Additional Controls | | | | | | | | |
| Test 2 | PP | 127 | - | Oxyfluorination[3] | APS | x | 70 | 7 |
| Test 3 | PP | 127 | - | - | APS | ✓ | 70 | 7 |
| Test 4 | PP | 127 | - | - | APS | x | 70 | 7 |

**Table I:** A summary of successful methods used to achieve a grafted layer of PNIPAAm onto the surfaces of poly(propylene) (PP), poly(ethylene terephthalate) (PET) and nylon non-woven polymers (light grey). The darker grey panel represents scaffolds of different pore sizes grafted as per PP-*g*-PNIPAAm-B and the darkest grey panel summarises the variations of grafting method PP-*g*-PNIPPAm-B to serve as additional controls for thermal release assessment.

### 2.4. Thermal release

Hepatocytes were cultured on all grafted scaffolds (5x5x3 mm; light grey shaded area in Table 1) for 10 days. On day 10 the scaffolds were gently rinsed in warm, sterile PBS to remove loose or dead cells and were placed (3/well) into a 6-well plate containing 2 mL of cooled (20°C) culture media. Nine scaffolds were used per grafting and sterilisation method: three scaffolds which remained in the incubator at 37°C, three at 20°C for 1 h and three at 20°C for 2 h to establish the length of time necessary for temperature-mediated cell detachment. The cell culture plates containing the scaffolds were periodically agitated by

gentle swirling during the incubations, where after the scaffolds were removed and the released cells on the bottom of the wells photographed at x40 magnification using a standard microscope (Olympus BX41).

## 3. Results

Grafting methods that yielded a layer of PNIPAAm on the surface of the non-woven fibres as verified by ATR-FTIR, DSC XPS and scanning electron microscopy (data not shown) are summarised in Table 1.

### 3.1. Cell viability and proliferation

The AB assay was performed to determine cell proliferation and viability of the HC04 and HepG2 hepatocytes within the various grafted and control scaffolds. Cells were observed to proliferate and their numbers increased over time on all the 3D control and grafted scaffolds (Fig. 1). The HC04 hepatocytes grown on the PP scaffolds had a first maximum on day 7 with a general decline in numbers on day 11. Cell numbers were observed to recover thereafter. This phenomenon was noted on all scaffolds regardless of the cell line except in a few instances e.g. HC04 cells growing in the Algimatrix™ alginate scaffolds and grafted nylon scaffolds. On the PP scaffolds the PP-*g*- PNIPAAm-1a and PP-*g*-PNIPAAm-B supported the highest number of HC04 hepatocytes; these results were comparable to the proliferation seen within the Algimatrix™ scaffold. HepG2 hepatocytes growing on PP scaffolds were best supported by PP-*g*-PNIPAAm-1, PP-*g*-PNIPAAm-1a and PP-*g*-PNIPAAm-B; these scaffolds supported more cells than the Algimatrix™ scaffold. HC04 and HepG2 hepatocytes growing on the PET scaffolds were, by comparison, better supported by the Algimatrix™ scaffold as well as the control scaffold. HepG2 hepatocytes did not

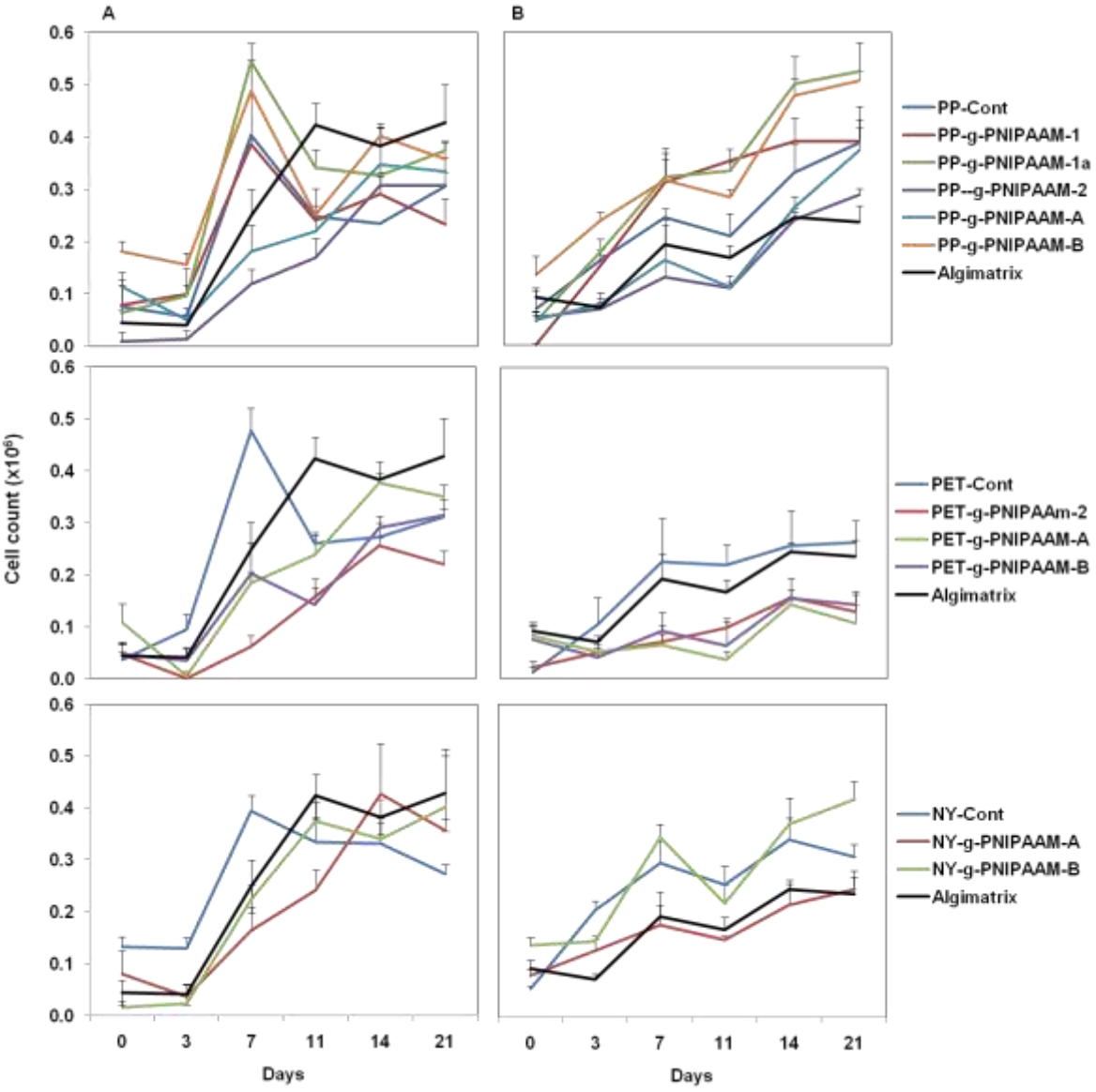


**Figure 1.** Cell proliferation on poly(propylene) (PP), poly(ethylene terephthalate) (PET) and nylon non-woven scaffolds, determined by the AB assay. HC04 (A) and HepG2 (B) hepatocyte cell lines growing on different scaffolds as summarised in Table 1 were assayed for viability and proliferation using AB on days 0 (hepatocyte retention in the scaffolds), 3, 7, 11, 14 and 21 and are represented as number of cells. The data are presented as the average of five individual scaffolds ± standard deviation.

proliferate well on the grafted PET scaffolds. Both cell lines grew well on the nylon scaffolds. HC04 hepatocytes grown on nylon-*g*-PNIPAAm-B matched the proliferation trend seen for the Algimatrix™ scaffold and, together with nylon-cont, surpassed the Algimatrix™ proliferation when supporting HepG2 hepatocytes.

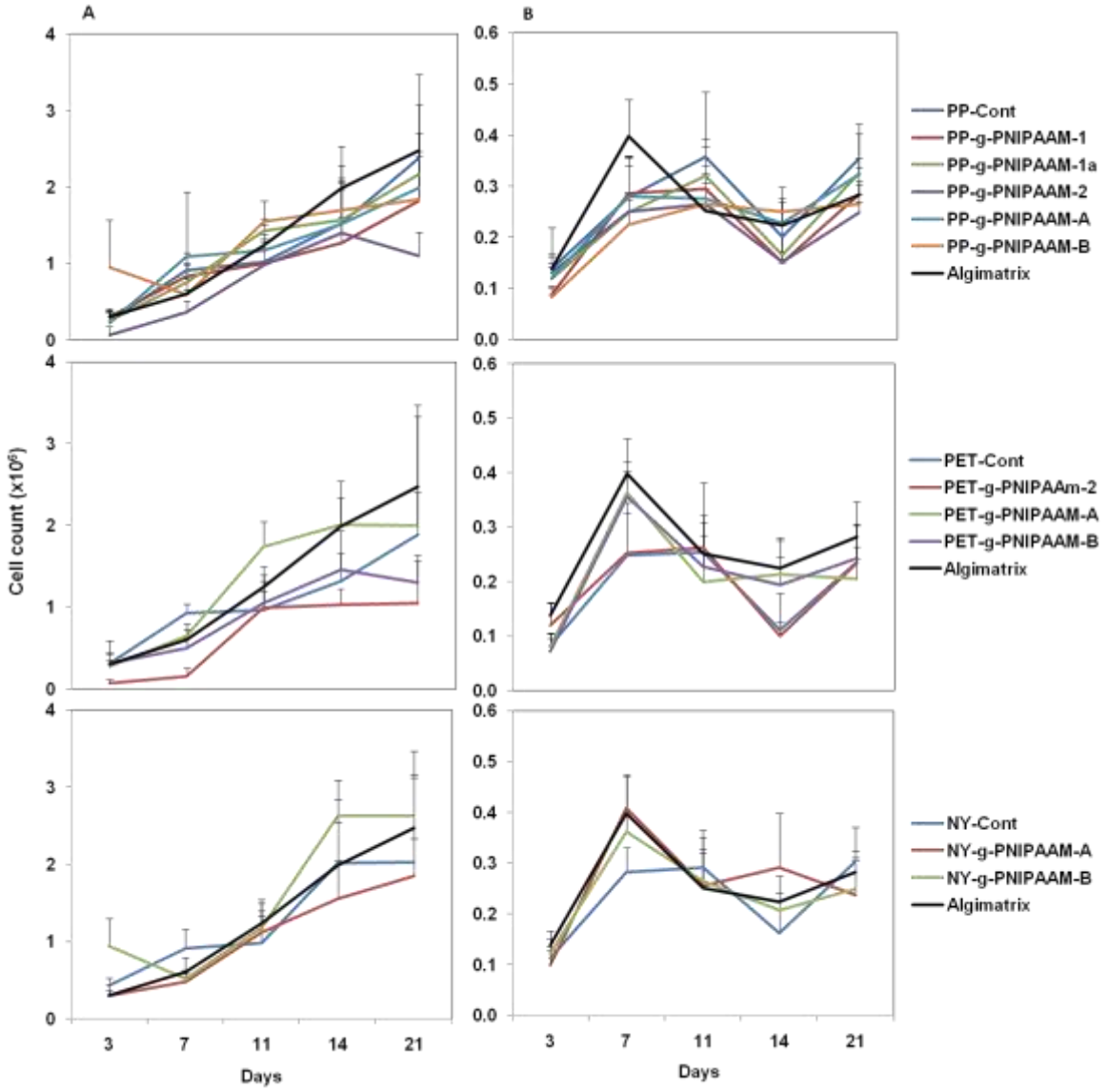


**Figure 2.** Cell proliferation of cell growing on poly(propylene) (PP), poly(ethylene terephthalate) (PET) and nylon non-woven scaffolds, determined by DNA staining. The proliferation of HC04 (A) and HepG2 (B) hepatocyte cell lines growing on different scaffolds as summarised in Table 1 was calculated using Hoechst 33258 fluorescence on days 3, 7, 11, 14 and 21. The data are presented as the average of five individual scaffolds ± standard deviation.

Total DNA was measured on days 3, 7, 11, 14 and 21 as an alternative means to measure cell proliferation on the 3D scaffolds. Cell numbers derived from the DNA quantification results indicated that up to 5-fold more HC04 hepatocytes, were growing on the scaffolds than suggested by the AB assay (Fig. 2). The HC04 hepatocytes growing on the PP, PET and nylon scaffolds showed an approximate linear increase in numbers over time, however, there

was not one scaffold that stood out as being far superior (or inferior) to the control scaffolds and Algimatrix™. Overall, DNA quantification-derived cell numbers of the HepG2 hepatocytes on the scaffolds more closely resembled the trend observed in the AB assay. As with the HC04 cells, no significant difference in growth on the grafted scaffolds as compared to the control scaffolds and Algimatrix™ (Fig. 2) was observed. A general decrease in HepG2 DNA levels was seen on day 11 on the PET and nylon scaffolds and on day 14 on the PP scaffolds after which DNA levels recovered or remained relatively constant.

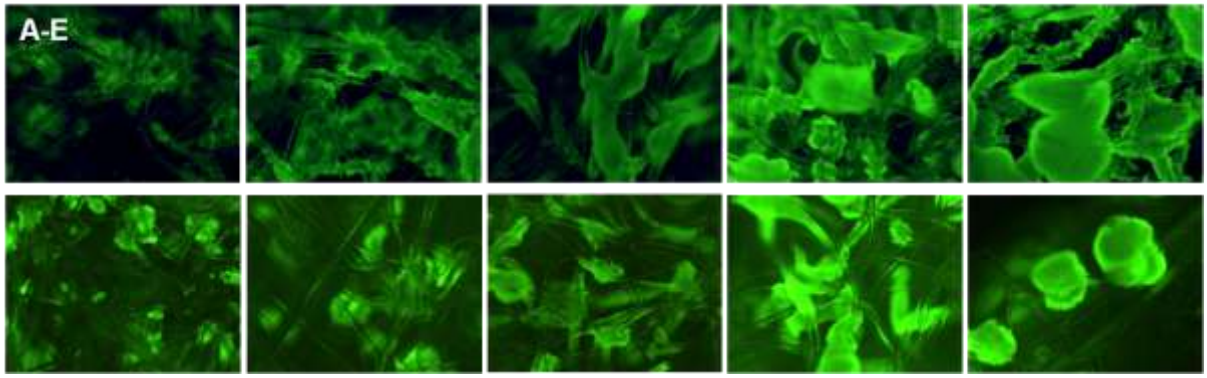


**Figure 3.** Representative fluorescence microscopy of HC04 (top panel) and HepG2 (bottom panel) cells growing on the PP-*g*-PNIPAAm-B scaffold after 3, 7, 11, 14 and 21 days (A-E) Cells were stained with Fluorescein Diacetate (FDA) and *v*isualisation was performed at 40x magnification using a standard fluorescence microscope (Olympus BX41) equipped with a 490 nm bandpass filter with a 510 nm cut-off filter for fluorescence emission.

Representative cell morphology and proliferation of the HC04 and HepG2 hepatocytes on the PP-*g*-PNIPAAm-B scaffold over 21 days is shown in Figure 3. HC04 hepatocytes grow along the non-woven fibres and at later time points form large cell clusters whereas the HepG2 hepatocytes have a greater tendency to form spheroids soon after seeding. Additionally, the metabolic activity of cells grown on a pure PP scaffold (mean pore size of 200 µm) was monitored as an indicator of viability and functionality. HC04 hepatocytes secreted on average twice the amount of albumin when cultured on the 3D PP non-grafted scaffolds as compared to the 2D monolayer, indicating that cells growing in the 3D context were more metabolically active than their 2D counterparts (Fig. 4). In contrast, the HepG2 cells took

longer to exceed the levels of albumin secreted by the 2D monolayer, achieving a maximum 1.5 -fold increase on day 21.

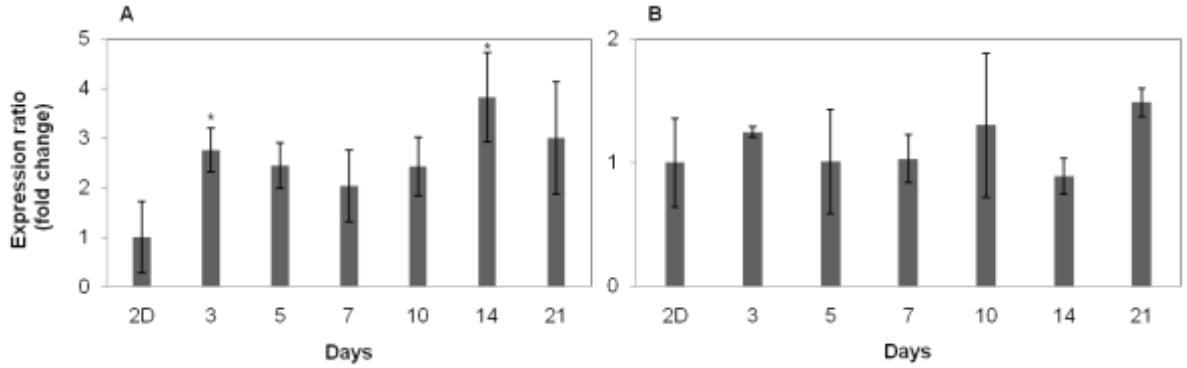


**Figure 4.** Relative albumin secretion in HC04 (A) and HepG2 (B) hepatocytes growing on a 3D non-woven control scaffold (pore size 200 µm). Known quantities of human albumin were used to establish a calibration curve and the quantities of albumin secreted into culture media were normalised to total protein levels in the media as determined by the Bradford assay to correct for differences in cell numbers. The data are indicated as fold change of cells growing in 3D compared to cells grown as a 2D monolayer. Data are the average of three individual scaffolds ± standard deviations; * indicates significance at $p<0.05$.

### 3.2. Cytochrome P450 mRNA expression

CYP gene expression was monitored using qRT-PCR in HC04 cells grown on the pure PP non-woven scaffolds with a mean pore size of 200 µm (Fig. 5A). CYP genes code for enzymes that are involved in the oxidation of organic compounds to enhance excretion and play a major role in the metabolism of drugs and xenobiotics. It has been hypothesised that hepatocytes growing in 3D may display enhanced drug metabolism due to higher levels of endogenous CYP gene expression. Expression levels of *CYP2C9, 2C19, 3A4* and *3A5* increased over time as the 3D scaffold became more densely populated, with *CYP1A2, 2C19* and *3A5*, up-regulated compared to the 2D control. *CYP2C19* for example, was expressed 79 times higher in the cells growing on the scaffold compared to the 2D control, using beta-actin as internal qRT-PCR reference control for cell numbers. For two genes, namely *CYP2C9* and *3A4*, levels of gene expression remained equal to, or below, that seen for HC04 cells grown

in 2D. This experiment revealed the highest level of CYP expression to be at day 21. On this basis, similar quantification of the selected CYP genes was performed at day 21 using HepG2 hepatocytes grown on the scaffold. CYP genes *1A2*, *2C9* and *2C19* were up regulated at day 21 while the expression levels of CYP genes *3A4* and *3A5* were less than that of the 2D control. *CYP2D6* was expressed at a similar level to that of the 2D control (Fig. 5B). When

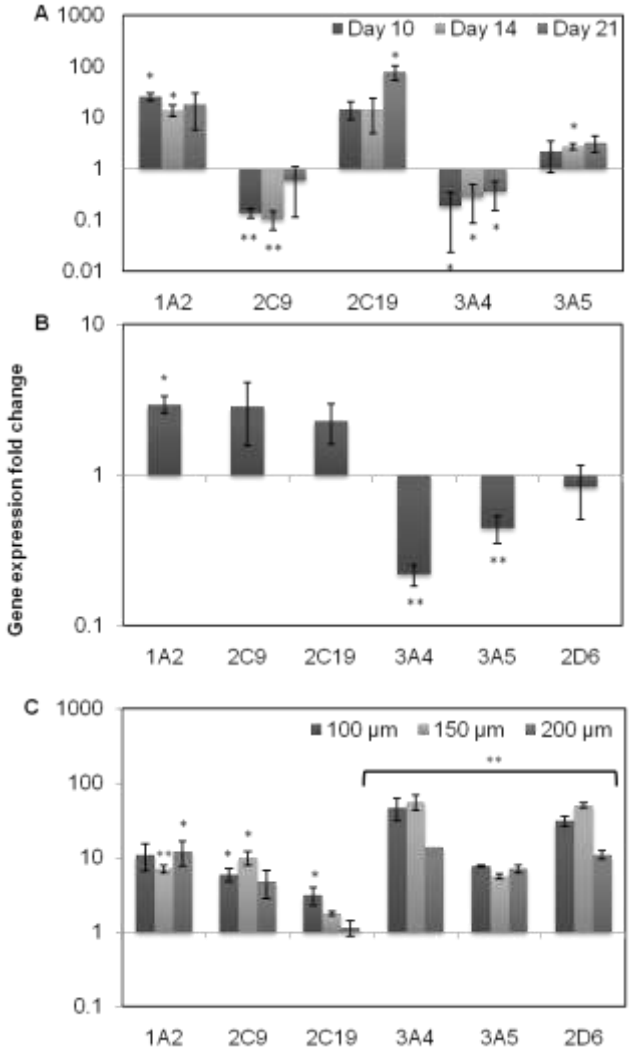


**Figure 5:** CYP gene expression. (A) HC04 hepatocyte CYP gene expression after 10, 14 and 21 days of growth on the non-grafted, 200 um pore size, poly(propylene) (PP) scaffolds. (B) HepG2 cytochrome gene expression after 21 days of growth on the same PP non-woven scaffolds as described for graph A. (C) HC04 cytochrome gene expression after 21 days of growth on scaffolds PP-*g*-PNIPAAm-B1 (100 µm), PP-*g*-PNIPAAm-B2 (150 µm) and PP-*g*-PNIPAAm-B3 (200 µm). Expression of each transcript, relative to a 2D HC04 monolayer culture, was determined using the $2^{-\Delta\Delta Ct}$ method by normalizing to β-actin expression and is graphed as fold induction compared to 2D. Data are represented as the average of three independent experiments performed in triplicate ± standard deviations. * indicates significance at $p< 0.05$ and ** indicates significance at $p<0.01$.

the CYP gene expression levels were assessed on scaffolds of different mean pore size that had been grafted (using grafting method of scaffold PP-*g*-PNIPAAm-B) it was noted that gene expression was increased for all the selected genes as depicted in Figure 5C. No specific conclusion can be drawn as to which pore size performed the best; however, the scaffolds PP-*g*-PNIPAAm-B1 (100 µm mean pore size) and PP-*g*-PNIPAAm-B2 (150 µm mean pore size) appeared to support higher levels of gene expression then PP-*g*-PNIPAAm-B3 (200 µm mean pore size).

### 3.3. Thermal release

An initial thermal release trial was conducted to ascertain which non-woven polymer, grafting and sterilisation method (autoclaving or ethanol) permits optimal cell release at 20°C using HC04 hepatocytes that had grown on the scaffolds for 10 days. Thermal release of HC04 hepatocytes at 20°C was observed most significantly after 2 h on the PP-*g*-PNIPAAm-A and PP-*g*-PNIPAAm-B scaffolds that had been ethanol sterilised (Fig. 6A). No other scaffold displayed significant thermal cell release. Although some scaffolds did appear to release cells, including PET-*g*-PNIPAAm-A (autoclaved, 1 h release), PET-*g*-PNIPAAm-B (ethanol, 2 h release) and nylon-*g*-PNIPAAm-A (autoclaved, 2 h release), these scaffolds were also observed to drop non-woven fibres, ruling out the possibility that thermal release alone was responsible for the released cells. This result was subsequently confirmed using HepG2 cells (Fig. 6B).

Additional controls were included to verify that none of the other components of the grafting process other than the presence of PNIPAAm was responsible for the observed cell release. Scaffold PP-*g*-PNIPAAm-B which had been oxyfluorinated and grafted displayed greater

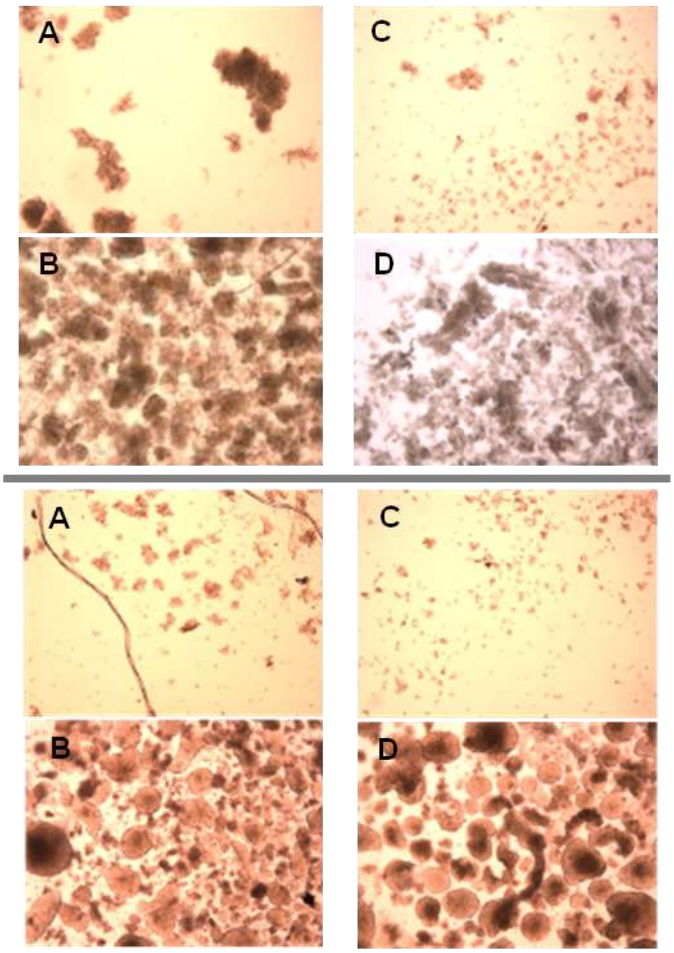


**Figure 6:** Thermal release of HC04 and HepG2 hepatocytes. Cells were grown on either PP-*g*-PNIPAAm-A (left hand panels) or PP-*g*-PNIPAAm-B scaffolds (right hand panels) for 10 days**.** Cell release was compared between scaffolds kept at 37 °C (A, C) or at 20°C (B, D) for 2 h for both HC04 (top panels, A-D) and HepG2 cells (bottom panels, A-D). Images of cells dropped from the scaffolds were taken using a standard microscope (Olympus BX41) at 40x magnification.

capacity for thermal release than the "test 2" and "test 4" scaffolds (Table 1), which had not been grafted with PNIPAAm. In addition scaffold PP-*g*-PNIPAAm-B released more cells than scaffold "test 3" which had been grafted but had no prior surface functionalisation i.e. oxyfluorination. It can thus be concluded that only the addition of PNIPAAm during the grafting procedure will result in release of cells from the scaffolds when the temperature is lowered below the LCST and that no other exogenous factors contribute to the observed cell release. In addition to this, grafted scaffolds with different pore sizes were tested to see if this had any affect on thermal release of the cells; after 10 days in culture it was observed that

pore size does not significantly affect cell release from the scaffolds with mean pore sizes of 100, 150 or 200 µm, based on visual estimation.

An estimation of cell recovery rates from the scaffolds was also conducted. Scaffolds PP-*g*-PNIPAAm-B1, PP-*g*-PNIPAAm-B2 and PP-*g*-PNIPAAm-B3 were seeded with hepatocytes; 14 days thereafter the number of total cells on the scaffolds was estimated using AB. Trypsin treatment of the scaffolds or thermal release was used to remove cells from the scaffolds (n=3). Viable cells released from the scaffolds were counted using trypan blue dye exclusion. Trypsin treatment of scaffolds PP-*g*-PNIPAAm-B1 and PP-*g*-PNIPAAm-B2 yielded approximately as many cells as the thermal release, however, more viable cells were released from PP-*g*-PNIPAAm-B3 after trypsin treatment than thermal release. In all instances with the exception of scaffold PP-*g*-PNIPAAm-B3 treated with trypsin (Table 2), fewer cells were released than the total estimated to be growing on the scaffold using AB thus indicating that neither trypsin nor thermal release is fully effective in releasing all the cells. Viable cells released from the scaffolds were seeded into a 6 well plate and assessed for re-attachment and growth as an additional indication of viability (data not shown).

| | **PP-*g*-PNIPAAm-B1** | **PP-*g*-PNIPAAm-B2** | **PP-*g*-PNIPAAm-B3** |
|---|---|---|---|
| Total Cells | 556 206 | 608 985 | 468 552 |
| Trypsin | 270 000 | 190 000 | 530 000 |
| Thermal Release | 230 000 | 230 000 | 250 000 |

**Table II:** Hepatocyte cell release from scaffolds PP-*g*-PNIPAAm-B1, PP-*g*-PNIPAAm-B2 and PP-*g*-PNIPAAm-B3 via trypsin treatment or thermal release. Total hepatocyte numbers on the scaffolds prior to cell release were estimated using AB. Viable cells released from the scaffolds were counted using trypan blue dye exclusion on a haemocytometer. The data are presented as the average of three individual scaffolds.

## 4. Discussion

A growing body of evidence has emerged where cells grown *in vitro* in 3D structures have been shown to be significantly different and more representative of the physiological state of the native source tissue than those grown in conventional 2D monolayer cultures. The development of new culturing systems that enhance this capability is therefore expected to lead to significant advances in the predictive accuracy of multiple *in vitro* cell culture applications, including the fundamental study of cell growth and signalling, host-pathogen interactions, and the drug discovery process. In this study, the need was identified to develop a scaffold which could not only support cell attachment and enhanced proliferation, but could furthermore be capable of releasing 3D cell structures non-invasively with surface and extracellular matrix proteins largely intact for downstream applications. This is the first report for the development of 3D, thermo-responsive, non-woven scaffolds able to release cells from a 3D matrix without the use of enzymatic detachment or degradation of the scaffold. The feasibility of using three different polymers for enhanced 3D cell culture, grafted by various means with PNIPAAm, was investigated.

AB and Hoechst 33258 were used independently for determining cell proliferation on the scaffolds as, to date, there is not one wholly accepted method for cell enumeration in 3D (Kee et al., 2005). For the majority of scaffolds tested with the AB assay, cell numbers, for both HC04 and HepG2 hepatocytes, were observed to initially increase after seeding but subsequently decline between days 7 and 11; thereafter cell numbers recovered and increased. Similar results have previously been observed by Shor and colleagues (2007) in the interaction of osteoblasts with polycaprolacton/ hydroxyapatite scaffolds. It has been suggested that this observed trend is due to the inability of the dye to penetrate the scaffolds

and react with the cells in the interior of the scaffolds. The recovery in cell numbers can be attributed to cells subsequently populating areas of the scaffold where the dye can more easily penetrate. The cell numbers estimated using the AB assay will not be accurately representative of the inner construct environment if a metabolite concentration gradient existed between the interior and the exterior of the construct and is therefore dependent on the efficiency of metabolite diffusion into and out of the construct. This can be overcome to a degree by swirling the wells containing the scaffolds during the incubation period to assist dye diffusion, however, this diffusivity of reagents into the 3D environment can ultimately become a confounding factor in this type of assay and it is thus important to use AB in combination with another cell quantification assay. The AB assay did, however, reveal that the cells were able to proliferate on the grafted scaffolds at a level comparable to, and in some instances better than that of the commercially available alginate scaffold, Algimatrix™ and the control scaffolds, suggesting an absence of scaffold-induced cytotoxicity.

The Hoechst 333258 assay indicated that the HC04 cells proliferated rapidly on the scaffolds whereas the growth of the HepG2 hepatocytes was relatively static over time. This can be largely attributed to the different way in which these cells grow. Fluorescence microscopy revealed that the HC04's displayed guided growth according to the non-woven fibre orientation forming 3D structures as depicted in Figure 3 and populating the majority of the scaffold surface area. HepG2 cells formed spheroids with a small area of attachment to the non-woven fibres soon after seeding into the scaffolds thus they did not populate the scaffolds as rapidly or as extensively as the HC04 cells. This discrepancy in morphology is also evident when looking at the images of cells liberated during thermal release (Fig. 6); HepG2 cells form definite spheroids whereas the released HC04 hepatocytes are in the form of long, multi-layered cell sheets and in some instances the imprint of the non-woven fibre

can be seen on the cell sheets. The disparity in the scaffold-associated HC04 cell numbers derived from the AB vs. DNA results may be attributable to differences in scaffold penetration of the respective reagents used. This discrepancy was not observed for HepG2 cells which do not populate the matrix as densely and may allow for more uniform reagent diffusion.

The albumin assay indicated that the cell lines are metabolically superior, when grown in 3D as compared to a conventional 2D monolayer, particularly in the case of HC04 cells. The comparison of 3D vs. 2D was carried out using an approximately 70% confluent 2D monolayer as this cell confluency is typically the benchmark used in conventional experimentation to represent the most optimal log phase of 2D hepatocyte growth. More mature, confluent 2D-cultured cells experience increased cellular stress and eventual cell death (Gómez-Lechón et al., 2000). Some fluctuation in albumin secretion was observed for both cell lines, which is not unusual (Gómez-Lechón et al., 2000) and Glicklis and colleagues (2004) also reported a decline in albumin production on day 7 in their 3D alginate scaffolds. Prestwich (2007) suggests a possible cyclic production of albumin, as well as urea and EROD activity of hepatocytes (primary and HepG2-C3A cells) cultured on hydrogel surfaces or in 3D by encapsulation in Extragel, a synthetic extracellular matrix; our data suggests this to be accurate. HepG2 3D cultures had lower levels of albumin production as compared to HC04 3D cultures. This may be as a result of restrictions on mass transfer of essential nutrients caused by the formation of spheroids. This was observed by Dvir-Ginzberg and colleagues (2004) when the spheroids in their alginate scaffolds reached sizes of 100 μm or larger. The compaction of the spheroids over time and the deposition of ECM proteins (Dvir-Ginzberg et al., 2004; Glicklis et al., 2000) could lead to the decreased ability to remove cell secretions

and reduce albumin levels in 3D HepG2 culture supernatants compared to the HC04 hepatocytes.

An additional indicator of superior hepatocyte growth on the scaffolds is increased CYP gene expression. Hepatocytes absorb drugs from the blood stream and metabolize them through phase-I and phase-II reactions (Hamilton et al., 2001). During phase-I metabolism, 90% of all drugs are oxidized by CYP isozymes with different substrate selectivities. Seven isoforms account for 95% of this activity namely 1A1, 1A2, 2C9, 2C19, 2D6, 2E1, and 3A4, with 3A4 responsible for over 65% of the metabolism of current therapeutic agents (Prestwich, 2007). Cytochrome isozymes are downregulated within 24 h after plating fresh hepatocytes onto conventional 2D tissue culture plastic (Prestwich, 2007), thus *in vitro* culture models that reflect the increased physiological CYP levels of primary hepatic tissues and cells are sought after in the pharmaceutical industry as surrogates for predicting *in vivo* phase I drug metabolism (Lübberstedt et al., 2011). In several instances the 3D non-woven scaffolds developed in this study promoted increases in CYP gene transcripts in both the HC04 and HepG2 cell lines relative to their respective monolayers. Gene expression increased in a time-dependent manner for the HC04 cells grown on the 200 µm pore size scaffolds that had not been grafted with PNIPAAm. Expression of the *CYP2C9* and *CYP3A4* isoforms, however, remained below that of the 2D monolayer cells. Similarly, after 21 days of growth on the non-grafted scaffolds, HepG2 cells displayed increased expression of three out of six CYP isoforms compared to 2D monolayer cells, while the remaining isoforms had levels of gene expression equivalent or less than that observed for the 2D monolayer. This contrasts with the results observed for the scaffolds grafted with PNIPAAm. All the CYP genes tested demonstrated increased levels of expression as compared to the 2D control on scaffolds with pores sizes 100 µm and 150 µm. This is a good indication that the grafted layer serves not

only as a mechanism for cell release from the scaffolds but positively influences hepatocyte growth and metabolism.

Two scaffolds with thermo-responsive properties were successfully developed, namely PP-*g*-PNIPAAm-A and PP-*g*-PNIPAAm-B. Large tracts of viable cells or spheroids were released from these scaffolds in a temperature-dependant manner and, by comparison with control scaffolds, this thermal release was shown to be exclusively caused by the grafted PNIPAAm layer. Fluorescent microscopy did, however, reveal that not all the cells were released from these thermo-responsive scaffolds. A comparison of thermal release versus trypsin treatment of the cells growing on scaffolds PP-*g*-PNIPAAm-B1 and PP-*g*-PNIPAAm-B2 revealed a similar efficiency in cell release from the scaffolds (Table 1). Scaffold PP-*g*-PNIPAAm-B3 however was more permissive to trypsin treatment possibly owing to the more open pore structure of the scaffold. The cells that remain in the scaffolds may either be trypsin resistant due to the 3D nature of the cell clusters or may not be been able to navigate out of the non-woven fibre network to be counted. Uneven grafting and scaffold areas devoid of PNIPAAm may be responsible for cells remaining on the scaffold. In addition, hepatocytes were, in some instances, observed to grow around the full circumference of the fibre, this means that when the phase transition of the PNIPAAm polymer triggers cell release it will simply repel the cells from the scaffold but not be sufficient for the the cells to separate from one another. It is for this reason that we believe some hepatocytes remain on the scaffold after the 2 h thermal release. Grafting efficiency and time for cell release are potential areas for further improvement. Currently the commercially available thermo-responsive 2D plates (UPCellTM, Cell Seed Inc, Tokyo, Japan) require just over 30 min for release of a monolayer of cells.

## 5. Conclusion

Poly(propylene), PET and nylon non-woven scaffolds grafted with PNIPAAm designed to serve as a new smart scaffold for use in 3D cell culture were tested *in vitro*. All the non-woven scaffolds, both grafted and pure supported hepatocyte attachment and proliferation; the proliferation data was comparable to that of the commercially available alginate scaffold, Algimatrix$^{TM}$. It is reported that cells growing in 3D on the grafted scaffolds had enhanced cytochrome gene expression as compared to cells growing on both the pure scaffolds and in 2D on tissue culture plastic; albumin production of cells in 3D was marginally enhanced over 21 days. We show detailed experiments testing the thermo-responsiveness of the various grafted scaffolds as compared to their controls; two scaffolds, namely, PP-*g*-PNIPAAm-A and PP-*g*-PNIPAAm-B were able to release viable cellular aggregates from the grafted scaffolds without mechanical scraping, scaffold degradation or the use of enzymes confirming the use of the grafted scaffolds in non-invasive 3D cell culture. This technology may find applications in the proliferation and non-invasive release of cells for long-term cell cryopreservation, bioreactor matrices or cell differentiation. Additional applications in host-pathogen studies and toxicology may also be optimized using the smart scaffold.

## Acknowledgements

The authors thank Rajesh Anandjiwala and Lydia Boguslavsky for preparing the non-woven fabrics. The funding for this work was provided by the Council for Scientific and Industrial Research.

**References**


Beningo KA, Dembo M, Wang Y-l. 2004. Responses of fibroblasts to anchorage of dorsal extracellular matrix receptors. Proc Natl Acad Sci U S A 101:18024-18029.

Bokhari M, Carnachan RJ, Cameron NR, Przyborski SA. 2007a. Culture of HepG2 liver cells on three dimensional polystyrene scaffolds enhances cell structure and function during toxicological challenge. J Anat 211:567-576.

Bokhari M, Carnachan RJ, Cameron NR, Przyborski SA. 2007b. Novel cell culture device enabling three-dimensional cell growth and improved cell function. Biochem Biophys Res Commun 354:1095-1100.

Cukierman E, Pankov R, Stevens DR, Yamada KM. 2001. Taking cell-matrix adhesions to the third dimension. Science 294:1708-1712.

Curti PS, de Moura MR, Veiga W, Radovanovic E, Rubira AF, Muniz EC. 2005. Characterization of PNIPAAm photografted on PET and PS surfaces. Appl Surf Sci 245:223-233.

Dvir-Ginzberg M, Elkayam T, Aflalo ED, Agbaria R, Cohen S. 2004. Ultrastructural and functional investigations of adult hepatocyte spheroids during *in vitro* cultivation. Tissue Eng 10:1806-1817.

Dvir-Ginzberg M, Gamlieli-Bonshtein I, Agbaria R, Cohen S. 2003. Liver tissue engineering within alginate scaffolds: Effects of cell-seeding density on hepatocyte viability, morphology, and function. Tissue Eng 9:757-766.

Glicklis R, Merchuk JC, Cohen S. 2004. Modeling mass transfer in hepatocyte spheroids via cell viability, spheroid size, and hepatocellular functions. Biotecnol Bioeng 86:672-680.

Glicklis R, Shapiro L, Agbaria R, Merchuk JC, Cohen S. 2000. Hepatocyte behavior within three-dimensional porous alginate scaffolds. Biotechnol Bioeng 67:344-353.

Gómez-Lechón MJ, Castell JV, Danato T, Pahernik S, Thasler W, H.G. K, Doser M, Dauner M, Planck H. 2000. New non-woven polyurethane-based biomaterials for the cultivation of hepatocytes: expression of differentiated functions. J Mater Sci Mater Med 11:37-41.

Hamilton GA, Jolley SL, Gilbert D, Coon JD, Barros S, LeCluyse EL. 2001. Regulation of cell morphology and cytochrome P450 expression in human hepatocytes by extracellular matrix and cell-cell interactions. Cell Tissue Res 306:85-99.

Kee NW, Leong DTW, Hutmacher DW. 2005. The challenge to measure cell proliferation in two and three dimensions. Tissue Eng 11 182-191.

Kushida A, Yamato M, Konno C, Kikuchi A, Sakarai Y, Okano T. 1999. Decrease in culture temperature releases monolayer endothelial cell sheets together with deposited fibronectin matrix from temperature-responsive culture surfaces. J of Biomed Mater Res 45:355-362.

Livak KJ, Schmittgen TD. 2001. Analysis of relative gene expression data using Real-Time Quantitative PCR and the $2^{-\Delta\Delta CT}$ method. Methods 25:402-408.

Lübberstedt M, Müller-Vieira U, Mayer M, Biemel KM, Knöspel F, Knobeloch D, Nüssler AK, Gerlach JC, Zeilinger K. 2011. HepaRG human hepatic cell line utility as a surrogate for primary human hepatocytes in drug metabolism assessment *in vitro*. J Pharmacol Toxicol Methods 63:59-68.

Okano T, Yamada N, Okuhara M, Sakai H, Sakurai Y. 1995. Mechanism of cell detachment from temperature-modulated, hydrophilic-hydrophobic polymer surfaces. Biomaterials 16:297-303.

Prestwich GD. 2007. Evaluating drug efficacy and toxicology in three dimensions: Using synthetic extracellular matrices in drug discovery. Acc. Chem. Res. 41:139-148.

Rago R, Mitched J, Wilding G. 1990. DNA fluorometric assay in 96-well tissue culture plates using Hoechst 33258 after cell lysis by freezing in distilled water. Anal Biochem 191:31-34.

Sainz B, TenCate V, Uprichard S. 2009. Three-dimensional Huh7 cell culture system for the study of Hepatitis C virus infection. Virol J 6:103.

Sattabongkot J, Yimamnuaychoke N, Leelaudomlipi S, Rasameesoraj M, Jenwithisuk R, Coleman RE, Udomsangpetch R, Cui L, Brewer TG. 2006. Establishment of a human hepatocyte line that supports *in vitro* development of the exo-erythrocytic stages of the malaria parasites *Plasmodium falciparum* and *P. vivax*. Am Journal Trop Med Hyg 74:708-715.

Schmeichel KL, Bissell MJ. 2003. Modeling tissue-specific signaling and organ function in three dimensions. J Cell Sci 116:2377-2388.

Shor L, Güçeri S, Wen X, Gandhi M, Sun W. 2007. Fabrication of three-dimensional polycaprolactone/hydroxyapatite tissue scaffolds and osteoblast-scaffolds interactions *in vitro*. Biomaterials 28:5291-5297.

Wagner WR, Muzzio DJ, Rilo HR, Deglau T, Ataai MM, Michalopoulos GK, Block GD. 1997. Effect of growth factors and defined medium on primary hepatocyte culture on polyester carriers with varying surface treatments. Tissue Eng 3:289-301.

Witte RP, Kao WJ. 2005. Keratinocyte-fibroblast paracrine interaction: the effects of substrate and culture condition. Biomaterials 26:3673-3682.

Yamato M, Utsumi M, Kushida A, Konno C, Kikuchi A, Okano T. 2001. Thermo-responsive culture dishes allow the intact harvest of multilayered keratinocyte sheets without dispase by reducing temperature. Tissue Eng 7:473-482.

Zhang S. 2004. Beyond the Petri Dish. Nat Biotechnol 22:151-152.

## Supplementary Table and Figures

| Gene | Accession number | Forward primer (5'→3') | Reverse Primer (5'→3') | Product length (bp) |
|---|---|---|---|---|
| CYP2C19 | NM_000769.1 | TGCACGAGGTCCAGAGATACAT | TTTAACGTCACAGGTCACTGCAT | 71 |
| CYP2C9 | NM_000771.3 | CCTGACTTCTGTGCTACATGACAA | ATTGCCACCTTCATCCAGAAA | 85 |
| CYP1A2 | NM_000761.3 | CTCCTCCTTCTTGCCCTTCA | GTTTACGAAGACACAGCATTTCTTG | 97 |
| CYP2D6 | NM_001025161.1 | TGTGCCCATCACCCAGATC | TCACGTTGCTCACGGCTTT | 95 |
| CYP3A4 | NM_017460.3 | GCAAGAAGAACAAGGACAACATAGAT | GCAAACCTCATGCCAATGC | 85 |
| CYP3A5 | NM_000777.2 | TGGGACCCGTACACATGGA | GACAAAACATTTCCCAACAAAGG | 81 |
| β-Actin | NNM_001101 | CCTGGCACCCAGCACAAT | GCCGATCCACACGGAGTACT | 70 |

**Supplementary Table I.** qRT-PCR cytochrome (CYP) primers sequences used quantify CYP gene expression in hepatocytes growing in 3D as compared to 2D monolayers.

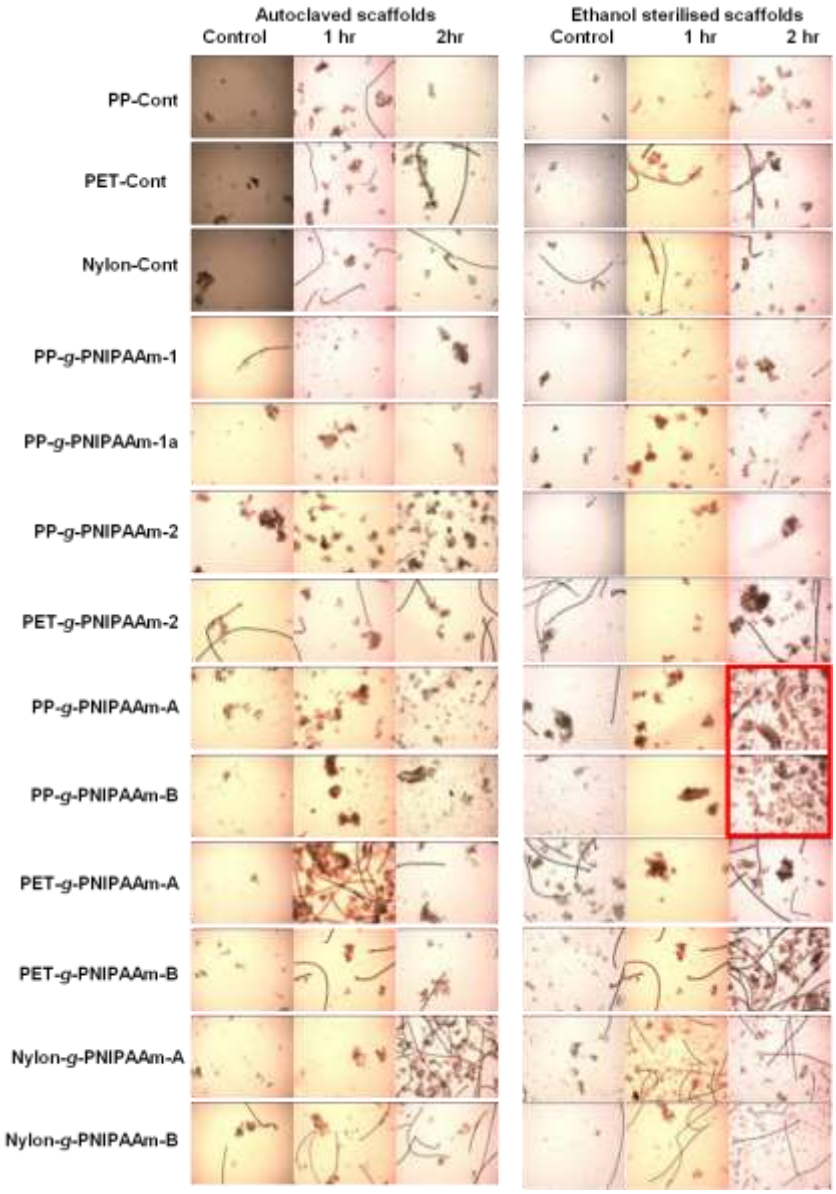


**Supplementary Figure 1:** Thermal release of HC04 hepatocytes from grafted and control scaffolds after 10 days of growth. Autoclaved and ethanol sterilised scaffolds were allowed to incubate at 37°C (control) and 20°C for 1 h and 2 h to assess the potential of each scaffold to undergo temperature induced cell release. The red box around PP-*g*-PNIPAAm-A and PP-*g*-PNIAPPM-B (both ethanol sterilised) after 2 h at 20°C indicates successful thermal release of the cells from the scaffolds as compared to their respective controls which were maintained at 37°C. Images of the dropped cells were taken using a standard microscope (Olympus BX41) at 40x magnification.

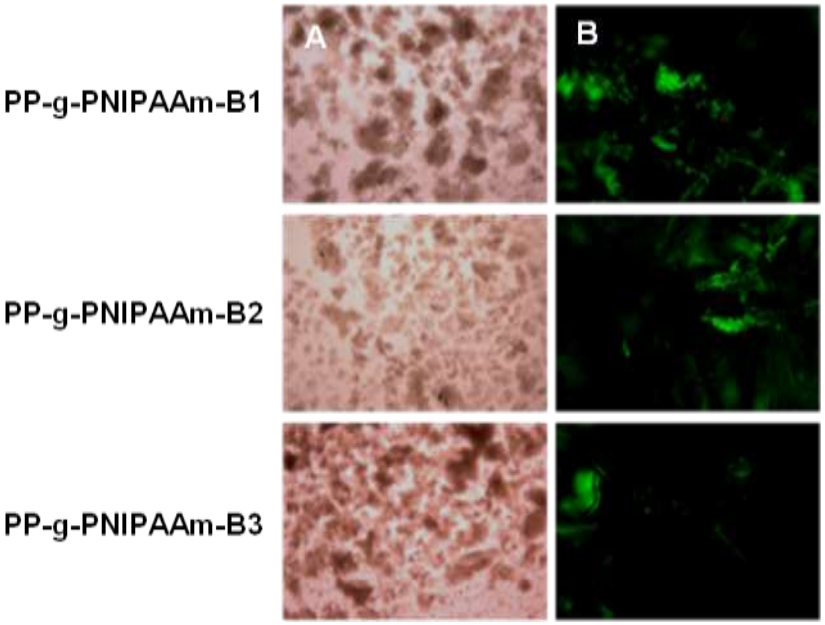


**Supplementary Figure 2.** Effect of non-woven scaffolds' pore size on thermal release. HC04 hepatocytes were released after 10 days of growth from ethanol sterilised scaffolds: PP-*g*-PNIPAAm-B1 (mean pore size 100 µm) PP-*g*-PNIPAAm-B2 (mean pore size 150 µm) and PP-*g*-PNIPAAm-B1 (mean pore size 200 µm) as summarised in Table 1 at 20°C for 2 hr. Images of the dropped cells were taken using a standard microscope (Olympus BX41) at 40x magnification. Fluorescent images of the cells remaining scaffolds after thermal release were taken using fluorescein diacetate (FDA, Sigma) using an Olympus BX41 microscope equipped with a 490 nm bandpass filter with a 510 nm cut-off filter for fluorescence emission.

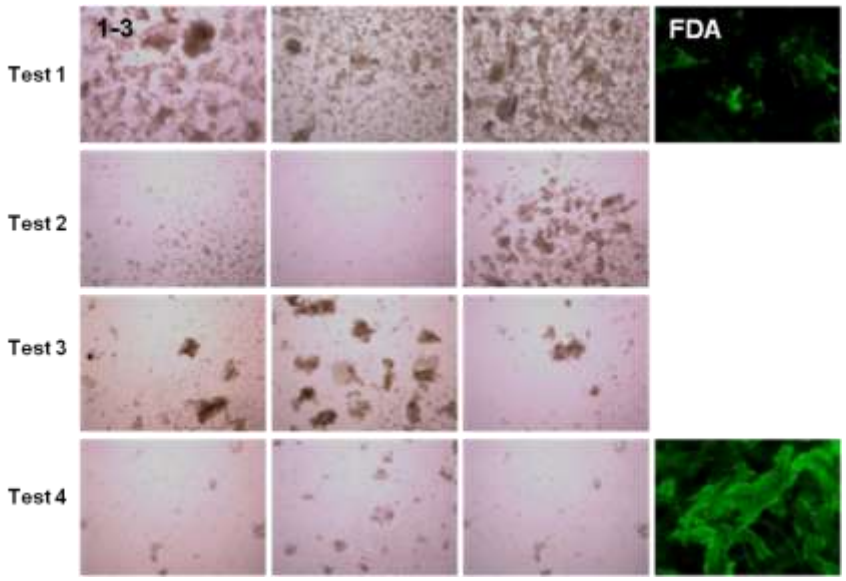


**Supplementary Figure 3:** Additional controls used to assess if omitting any stages of the grafting process have any effect on thermal release. Panels 1-3 are HC04 hepatocytes dropped from biological replications of each of the grafting variations, Test 1 – Test 4 as summarised by Table 1. Thermal release of cells that had been growing on ethanol sterilised scaffolds (Test 1-4) for 10 days took place at 20°C for 2 hr. Thermal release images of the dropped cells were taken using a standard microscope (Olympus BX41) at 40x magnification. HC04 hepatocytes remaining on the scaffolds Test 1 (grafted) and Test 4 (not grafted) after thermal release were visualised using Fluorescein diacetate (FDA, Sigma-Aldrich Chemie) at 40x magnification using an Olympus BX41 microscope equipped with a 490 nm bandpass filter with a 510 nm cut-off filter for fluorescence emission.